JACS
JOURNAL OF THE AMERICAN CHEMICAL SOCIETY

Article

pubs.acs.org/JACS

Highly Robust Hybrid Photocatalyst for Carbon Dioxide Reduction: Tuning and Optimization of Catalytic Activities of Dye/TiO_2/Re(I) Organic–Inorganic Ternary Systems

Dong-Il Won, Jong-Su Lee, Jung-Min Ji, Won-Jo Jung, Ho-Jin Son,* Chyongjin Pac,* and Sang Ook Kang*

Department of Advanced Materials Chemistry, Korea University, Sejong 30019, Korea

Supporting Information

ABSTRACT: Herein we report a detailed investigation of a highly robust hybrid system (sensitizer/TiO_2/catalyst) for the visible-light reduction of CO_2 to CO; the system comprises 5′-(4-[bis(4-methoxymethylphenyl)amino]phenyl-2,2′-dithiophen-5-yl)cyanoacrylic acid as the sensitizer and (4,4′-bis(methylphosphonic acid)-2,2′-bipyridine)$Re^{I}(CO)_3Cl$ as the catalyst, both of which have been anchored on three different types of TiO_2 particles (s-TiO_2, h-TiO_2, d-TiO_2). It was found that remarkable enhancements in the CO_2 conversion activity of the hybrid photocatalytic system can be achieved by addition of water or such other additives as Li^+, Na^+, and TEOA. The photocatalytic CO_2 reduction efficiency was enhanced by approximately 300% upon addition of 3% (v/v) H_2O, giving a turnover number of ≥570 for 30 h. A series of Mott–Schottky (MS) analyses on nanoparticle TiO_2 films demonstrated that the flat-band potential (V_{fb}) of TiO_2 in dry DMF is substantially negative but positively shifts to considerable degrees in the presence of water or Li^+, indicating that the enhancement effects of the additives on the catalytic activity should mainly arise from optimal alignment of the TiO_2 V_{fb} with respect to the excited-state oxidation potential of the sensitizer and the reduction potential of the catalyst in our ternary system. The present results confirm that the TiO_2 semiconductor in our heterogeneous hybrid system is an essential component that can effectively work as an electron reservoir and as an electron transporting mediator to play essential roles in the persistent photocatalysis activity of the hybrid system in the selective reduction of CO_2 to CO.

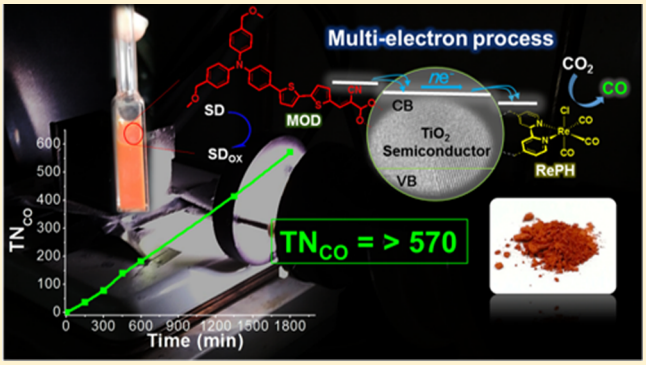

INTRODUCTION

Development of CO_2 reduction catalysts has attracted considerable interest because of the global climate change that has been caused by the rapid increase in CO_2 concentration (the most abundant greenhouse gas) in the atmosphere as a result of burning fossil fuels.[1−4] A potential response to this problem is the use of solar-light-driven reduction of CO_2 to fuels or other useful chemicals, which is one of the major objectives of artificial photosynthesis.[5−8] It is a general consensus in the field of artificial photosynthesis that proton-coupled multielectron reductions of CO_2 should be adopted as low-energy processes, as the one-electron reduction of CO_2 to $CO_2^{\bullet-}$ can occur only at very negative potentials.[9−12] Such low-energy processes require suitable catalysts, among which transition-metal complexes have been regarded as potential candidates for artificial photosynthesis[13−15] and electrochemistry,[16,17] because of the easy tuning of their redox potentials, trapping of CO_2 via coordination to the metal center, and valence jump of the metal oxidation state in response to multielectron reduction processes.[18−21] Among transition-metal-based system for CO_2 reduction, the (bpy)-$Re^{I}(CO)_3Cl$ (bpy = 2,2′-bipyridine) complex demonstrated initially by Lehn and co-workers[22,23] is of great interest due to the its highly selective photoreduction of CO_2 to CO in excellent efficiencies.

A general scheme for artificial photosynthetic CO_2 reduction involves visible-light-driven electron transfer followed by proton-coupled, multielectron processes to yield stable CO_2-reduction products.[13,17,24] Therefore, possible reaction systems for CO_2 reduction should minimally consist of a visible-light-harvesting antenna, a suitable electron donor–acceptor pair, an effective electron-transporting path, and a catalyst capable of reducing CO_2 with the transported electrons. As such, a ternary hybrid system formed by loading both a dye and catalyst onto n-type semiconductor nanoparticles would potentially be usable. In such a system, the semiconductor should function as an efficient electron acceptor for the photoexcited dye, a pool capable of storing multiple electrons, and a path for transporting electrons to the catalyst. However, construction of

Received: August 21, 2015
Published: October 10, 2015

DOI: 10.1021/jacs.5b08890
J. Am. Chem. Soc. 2015, 137, 13679−13690

Chart 1. Electron Donor, Sensitizer, and Reduction Catalyst Used for Hybrid System

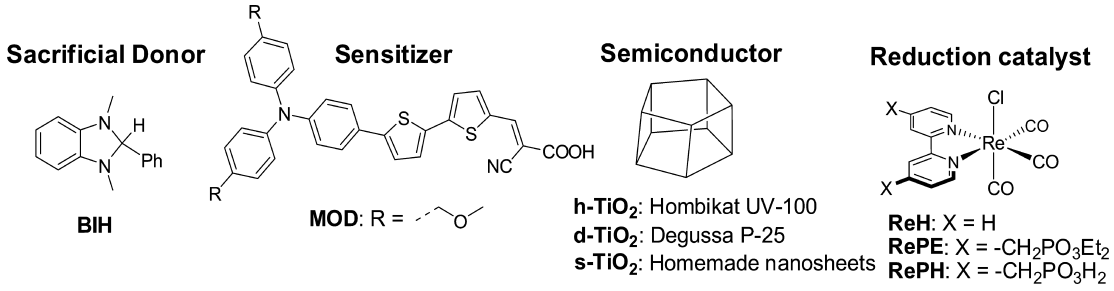

Scheme 1. Synthesis Routes of Reduction Catalysts (ReH, RePE, and RePH) and Sacrificial Donor Molecule (BIH)

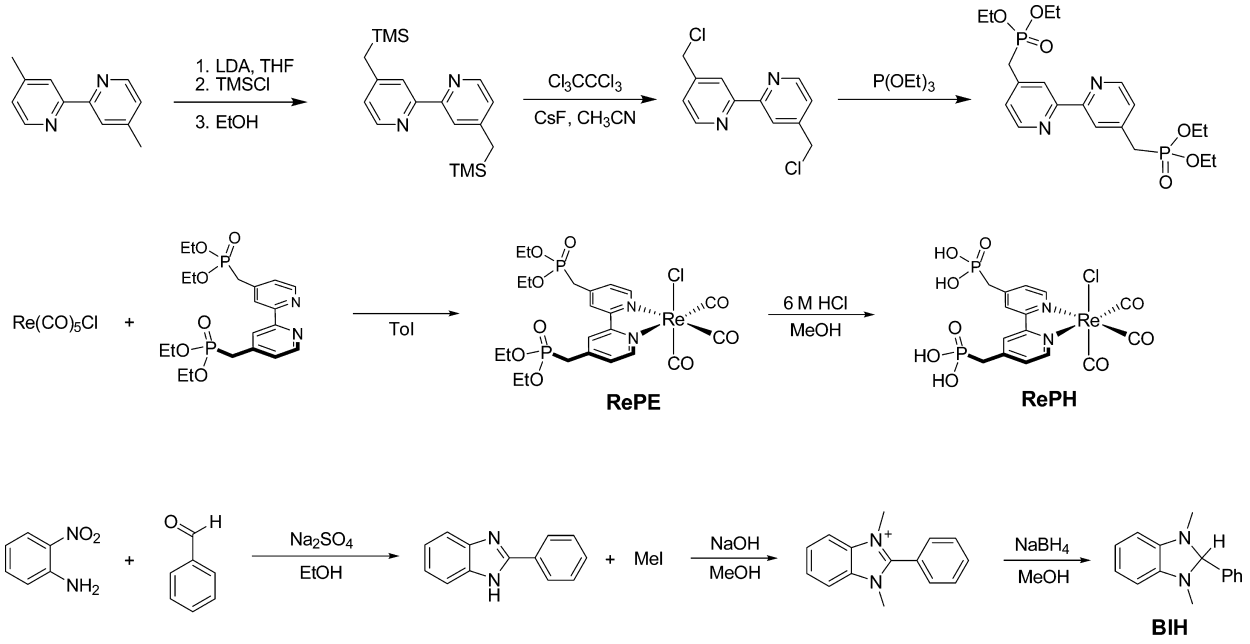

effective hybrid systems requires that the relative potential levels of the components be adjusted to allow for electron flow from the excited-state dye to the catalyst through the semiconductor. Furthermore, it should be considered that other complex factors may participate in controlling the photocatalytic behavior of a given hybrid system, including the characteristics of the semiconductor (e.g., conduction-band edge, morphologies, particle sizes, and trap-site distributions), molecular densities of the dye and catalyst anchored on the semiconductor, chemical reactivity of the catalyst, solid–solution interface properties, and effects of other molecules present in the solution. While some interesting reports on photocatalytic CO_2 reduction using molecule–semiconductor hybrids have been reported,[25−31] there have been few systematic investigations to explore the essential factors controlling the photocatalytic functions of hybrid systems.

In a previous communication,[32] we reported that hybrids containing organic dyes and $[(L)Re(CO)_3Cl]$ complexes anchored on TiO_2 nanoparticles exhibited persistent photocatalytic behavior in the selective reduction of CO_2 to CO in *N*,*N*-dimethylformamide (DMF) using a dihydrobenzimidazole derivative as the sacrificial electron donor (BIH) (Chart 1). The preliminary investigation showed that the photocatalytic efficiencies were substantially affected by the sources of the TiO_2 particles, the sequences of anchoring the dye and catalyst, and the addition of triethanolamine (TEOA) or Brønsted acids, typically water.[32] These versatile features might provide useful clues to understanding the chemical essence of the hybrids associated with their catalytic functions, thus facilitating optimization of the photocatalytic activity. In this paper, we report the details of photocatalytic CO_2 reduction performed under various conditions and discuss the property–reactivity relationships based on the relative flat-band potentials (V_{fb}) of TiO_2 under various conditions.

RESULTS

Materials. Chart 1 shows the materials used in the present work, involving the donor–acceptor-type dye with the cyanoacrylic acid anchoring group (MOD) as photosensitizer, Re(I) complexes (ReH, RePE, and RePH) as CO_2-reduction catalyst, three different types of TiO_2 particles (h-TiO_2, d-TiO_2, and s-TiO_2), and 1,3-dimethyl-2-phenyl-1,3-dihydrobenzimidazole (BIH) as sacrificial electron donor. The organic sensitizer was prepared according to the method reported in a previous paper.[33,34] The synthesis of RePE/RePH[32,35,36] and BIH[37] was performed according to Scheme 1 following published methods. RePH was anchored on TiO_2 particles through the methylene-bridged phosphonic acid substituents of the bipyridine ligand for the construction of hybrid systems, whereas ReH and RePE were used as the catalyst for homogeneous photoreactions as comparative experiments. Tables S1 and S2 summarize the photophysical and electro-

DOI: 10.1021/jacs.5b08890
J. Am. Chem. Soc. 2015, 137, 13679−13690

chemical properties of the dyes and Re(I) complexes, and Figures S1 and S2 show the absorption and emission spectra of the Re(I) complexes in THF.

The TiO_2 materials used in this study are Hombikat UV-100 (100% anatase, h-TiO_2), Degussa P-25 (ca. 25% rutile and 75% anatase, d-TiO_2), and homemade TiO_2 nanosheets (s-TiO_2) obtained by treatment of [001] facet-exposed TiO_2[38] with 0.1 M NaOH aqueous solution.[39] The alkaline treatment was indispensable for efficient deposition of both RePH and MOD on the particles because the fluorinated surface of the as-prepared [001] TiO_2 is highly inert to anchoring of the dye and catalyst. All the TiO_2 materials were washed with deionized water under sonication prior to use. Figure 1 shows TEM

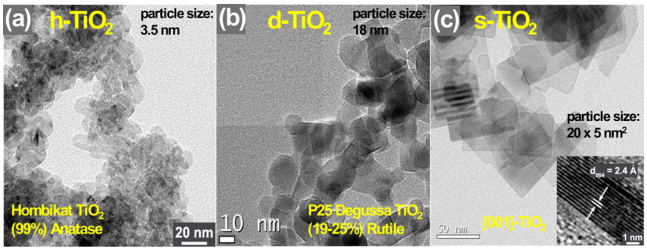

Figure 1. TEM images for h-TiO_2 (a), d-TiO_2 (b), and s-TiO_2 (c). Average sizes are 5 nm for h-TiO_2, 18 nm for d-TiO_2, and 20 nm (length) × 5 nm (thickness) for square-shaped nanosheet s-TiO_2 with ≈90% [001] facets. Inset in (c) shows the *d*-spacing of the (004) plane which is 2.4 Å, consistent with the values of the anatase phase bulk (JCPDS No. 21-1272; tetragonal a = 3.785 Å and c = 9.513 Å).

images of the TiO_2 materials, revealing different sizes and morphologies of the nanoparticles used. The specific Brauner–Emmett–Teller (BET) surface areas were determined to be >250 m^2/g for h-TiO_2, 50 m^2/g for d-TiO_2, and 110 m^2/g for s-TiO_2. Anchoring of RePH and MOD on the TiO_2 particles can be easily achieved by treatments of the TiO_2 particles with each solution of RePH and MOD (for details, see Experimental Section). The hybrid particles were isolated by centrifugation. The supernatant obtained by centrifugation after each adsorption treatment was confirmed to be transparent, indicating the complete adsorption of the components. Consequently, we assume that the amounts of RePH and MOD anchored on TiO_2 equal those present in the solutions used for adsorption, which are 0.1 and 1.5 μmol on 10 mg TiO_2, respectively, in the present investigation. The hybrids are abbreviated as RePH/TiO_2/MOD when RePH has been initially loaded and MOD/TiO_2/RePH when the dye has been initially loaded.

Photocatalytic CO_2 Reduction. Dispersions of the hybrid particles (10 mg of dye/TiO_2/catalyst or catalyst/TiO_2/dye) in 3 mL of CO_2-saturated DMF containing 0.1 M BIH were irradiated at >420 nm using a xenon lamp coupled with a cutoff optical filter. Analysis of gaseous product(s) evolved in the overhead space of the reaction vessel was undertaken by gas chromatographic analysis (GC), whereas the liquid phase after irradiation was analyzed by HPLC. For all photoreactions, it was confirmed that the exclusive product is commonly CO accompanied by a trace amount of H_2, while formic acid was not detected at all. Figure 2A shows plots of turnover numbers for CO formation (TN_{CO}) versus irradiation time for the MOD/h-TiO_2/RePH hybrid-dispersion system; TN_{CO} represents mole numbers of CO formed relative to unit mole of the Re(I) catalyst used. The CO formation steadily continued up to ~20 h with no leveling-off tendency. It was confirmed that the codeposition of both MOD and RePH on TiO_2 is indispensable for the efficient formation of CO seen in Figure 2A, since MOD/h-TiO_2 or h-TiO_2/RePH without anchoring of either RePH or MOD was much less efficient at formation of CO (see Figure S5 in Supporting Information). The much lower rate of photocatalytic CO_2 reduction for MOD/ZrO_2/RePH compared to MOD/h-TiO_2/RePH shows that the ET mechanism from MOD to RePH through the TiO_2 particle is preferential with TiO_2 but not with ZrO_2, due to the energetic mismatch between MOD* and the CB of ZrO_2. This result, in turn, indicates that our hybrid system has low possibility of direct ET between MOD and RePH on semiconductor particle (see Figure 2A).

$$\mathrm{AQY} = \frac{2 \times \text{amount of CO generated per unit time}}{\text{number of incident photons per unit time}} \quad (1)$$

The apparent quantum yield (AQY) of CO formation at 436 nm for the hybrid system (MOD/h-TiO_2/RePH) in the presence of 3% water was determined to be (2.14 ± 0.06) × 10^{-2}. As defined in eq 1, the measured AQY is not the real quantum yield with scientific definition but represents a relative

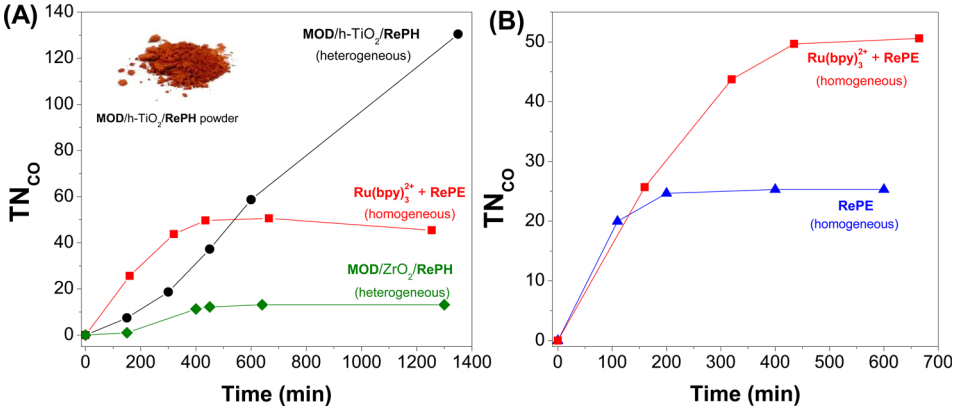

Figure 2. Plots of CO formation (TN_{CO}) versus time for CO_2-saturated DMF solution (3 mL) under various conditions. (A) MOD (1.5 μmol)/h-TiO_2 (10 mg)/RePH (0.1 μmol) (●), $Ru(bpy)_3^{2+}$ (0.1 mM) + RePE (1.0 mM) (red ■), and MOD (1.5 μmol)/ZrO_2 (10 mg)/RePH (0.1 μmol) (green ◆) in the presence of 0.1 M BIH irradiated at >420 nm (■). (B) RePE (1.0 mM) (blue ▲) and $Ru(bpy)_3^{2+}$ (0.1 mM) + RePE (1.0 mM) (red ■) in the presence of 0.1 M BIH irradiated at >420 nm.

DOI: 10.1021/jacs.5b08890
J. Am. Chem. Soc. 2015, 137, 13679–13690

estimate for the utilization efficiency of photogenerated electrons into CO formation with respect to the incident light intensity because the number of photons absorbed by the sensitizer cannot be exactly determined. The relatively low AQY appears to arise, at least in part, from poor light harvesting by the dye due to extensive light scattering in the particle dispersion system.

An isotope-labeling experiment was undertaken for MOD/h-TiO_2/RePH dispersions in $^{13}CO_2$-saturated DMF-d_6. As shown in Figure 3, the ^{13}C NMR spectrum of the irradiated sample

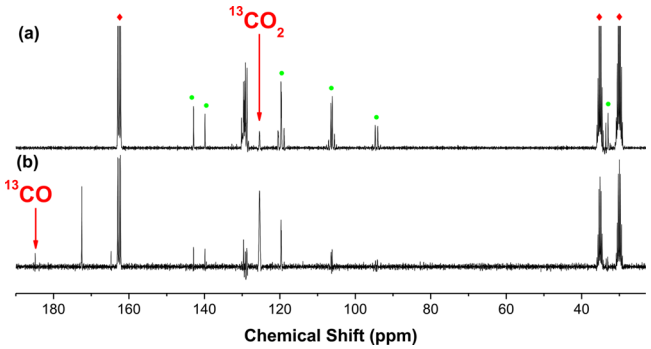

Figure 3. ^{13}C NMR spectra before (a) and after (b) irradiation. DMF-d_7 containing 10 mg of MOD/h-TiO_2/RePH dispersion in CO_2-saturated BIH (0.1 M); irradiation at >420 nm. The symbols ♦ and ● represent the peaks of DMF and BIH, respectively.

reveals a sharp signal at δ 185.2 ppm corresponding to the resonance of ^{13}CO. Moreover, the ^{13}C isotope abundance in the CO formed was analyzed by GC-MS to be >90% (Figure S9). It is therefore evident that CO_2 is the source of CO formed.

For comparison, photoreactions of homogeneous system were performed for solutions of RePE in CO_2-saturated DMF containing BIH as sacrificial donor under irradiation at >400 nm where the Re(I) complex was excited to work as both light absorber and CO_2-reduction catalyst or at >420 nm where $Ru(bpy)_3^{2+}$ (bpy = 2,2′-bipyridine) was used as visible-light sensitizer. In contrast to the hybrid-photocatalyzed reaction, the CO formation commonly shows leveling-off tendencies after 100 or 400 min irradiation to give lower TN_{CO} (Figure 2B). The leveling-off behavior is a general phenomenon observed in most reported investigations on homogeneous photocatalytic CO_2 reductions by ReH and related Re(I) complexes[22,23,40−42] with a few exceptions,[43−47] a consequence arising from chemical changes of the Re(I) catalysts.[48−50] As shown in Figure 4, on the other hand, IR spectra of the hybrid particles recovered after the photoreactions for 50 min, 100 min, and 20 h indicate no significant difference in the CO absorption bands of RePH, demonstrating that RePH does work as a persistent, stable catalyst in the reduction of CO_2 to CO with little decomposition after its anchoring on TiO_2. Regarding a little shifting of CO stretching vibrations (2025 to 2020 cm^{-1}), it is thought that the increase of electron density of rhenium center (with electron supply from MOD/TiO_2 during photoreaction) probably lowers the energy of the carbonyl stretching vibrations.

It has been well established that the photocatalytic CO_2 reduction by Re(I) complexes proceeds under participation of various intermediates and reactive species (e.g., one-electron reduced molecule, 17-electron species, and CO_2-coordinated molecules of the Re complexes), which are relatively long-lived.

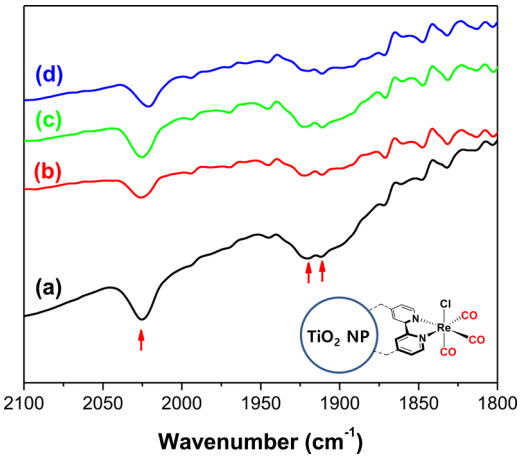

Figure 4. IR spectra of MOD/h-TiO_2/RePH in KBr disks (sample:KBr ≈ 1:100) before (a), after irradiation for 50 min (b), 100 min (c), and for 20 h (d). Red arrows indicate the absorptions of the CO ligands of RePH.

In homogeneous solution, these species are unintentionally distributed and diffusively encounter each other to undergo unfavorable reactions, which lead to yet fully unspecified chemical changes of the starting complex. In the hybrid system, RePH molecules anchored on TiO_2 should be separated far from each other enough to avoid intermolecular interactions so that each catalyst site might be able to exhibit its own inherent capability for the two-electron CO_2 reduction under steady supply of electrons through TiO_2.

The other hybrid systems using s-TiO_2 and d-TiO_2 are also effective at steady formation of CO, but with different efficiencies, as shown in Figure 5. An interesting observation is that the hybrid prepared by the initial loading of MOD (i.e., MOD/s- or d-TiO_2/RePH) shows a sizable higher catalytic activity compared to RePH/s- or d-TiO_2/MOD prepared by the initial loading of RePH, whereas the loading-sequence effect is nominal in the case of h-TiO_2. Table S3 summarizes TN_{CO} values after 10 h irradiation for the different hybrids. The loading-sequence effects appear to be related with differences in the size and morphology of primary particles, i.e., larger-size square-shaped nanosheet s-TiO_2 with exposed [001] facets (20 nm length ×5 nm thickness), 20 nm particulate d-TiO_2, and much smaller particulate h-TiO_2 (3.5 nm). Presumably, the surfaces of larger-size s- and d-TiO_2 would have local distributions with different activities in the electron injection from excited-state MOD into TiO_2, in charge recombination between an injected electron and $MOD^{\bullet+}$, in the transfer of injected electrons to RePH, and/or in chemical processes of CO_2 reduction on the RePH site. In the case of smaller-size pure anatase h-TiO_2, on the other hand, the surface would be relatively homogeneous so that the electron-transfer and chemical processes might proceed independently of the anchored locations.

Additive Effects. It was found that the photocatalytic activities of the hybrid systems are considerably affected by such additives as water, lithium perchlorate, sodium perchlorate, and TEOA. Detailed investigations were mainly performed on the MOD/h-TiO_2/RePH hybrid system. Figure 6 shows plots of TN_{CO} versus irradiation time for MOD/h-TiO_2/RePH in the absence and presence of 3% (v/v) H_2O. The CO formation was dramatically enhanced in the presence of H_2O, giving TN_{CO} of ∼200 after 10 h irradiation which is ∼3

DOI: 10.1021/jacs.5b08890
J. Am. Chem. Soc. 2015, 137, 13679−13690

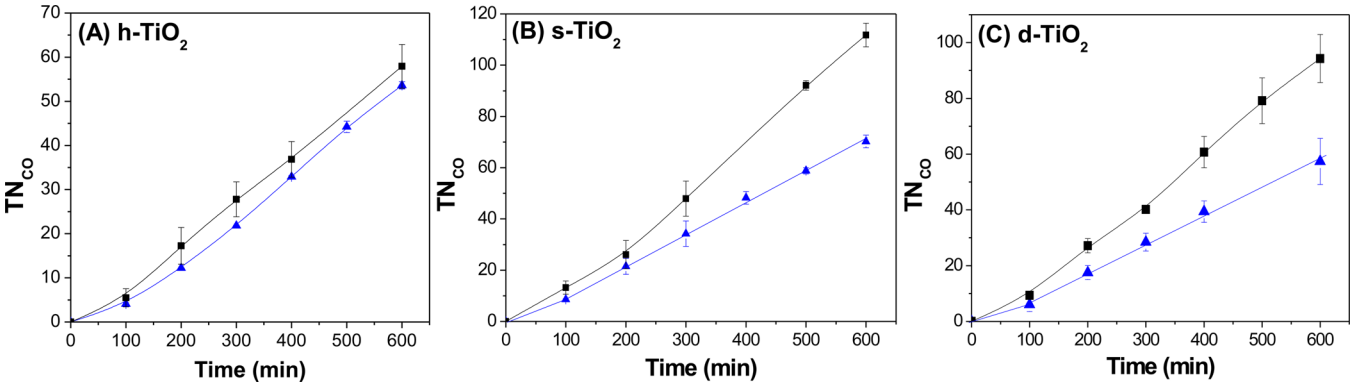

Figure 5. Time courses of CO formation by irradiation at >420 nm for MOD/TiO_2/RePH (■) and RePH/TiO_2/MOD (blue ▲), respectively (TiO_2 = h-TiO_2 (A), s-TiO_2 (B), and d-TiO_2 (C)); 10 mg of the hybrids with 0.1 μM RePH and 1.5 μM MOD in 3 mL of DMF in the presence of 0.1 M BIH.

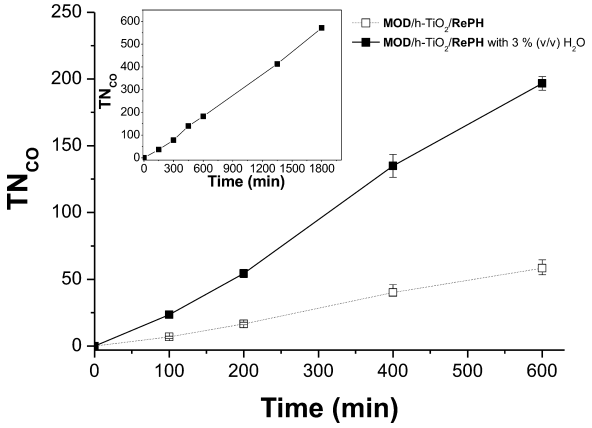

Figure 6. Plots of CO formation versus time for MOD/h-TiO_2/RePH in the absence (□) and presence of 3% (v/v) H_2O (■) in CO_2-saturated DMF containing 0.1 M BIH; irradiation at >420 nm. Inset shows formation of CO in the presence of 3% (v/v) H_2O by extended irradiation for 30 h.

times higher than that without addition of H_2O; TN_{CO} in the presence of 3% (v/v) H_2O continuously increases by 30 h to reach 570 with no appreciable leveling-off tendency (Figure 6 (inset)). Lithium perchlorate reveals unique, concentration-dependent enhancement effects, as shown in Figure 7 (also see Figure S7 in the Supporting Information). The maximum effect

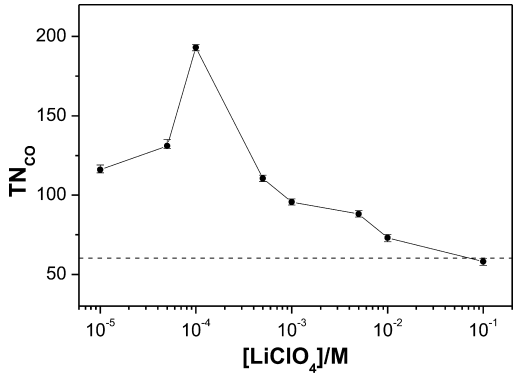

Figure 7. Dependence of TN_{CO} on concentration of $LiClO_4$ for 10 mg of MOD/h-TiO_2/RePH in 3 mL of CO_2-saturated DMF containing 0.1 M BIH irradiated at >420 nm for 10 h. The broken horizontal line indicates TN_{CO} in the absence of $LiClO_4$.

was observed at a low concentration (100 μM). Sodium perchlorate is another effective additive but can enhance the photocatalyzed CO formation at a relatively high concentration (0.1 M). We also examined possible effects of TEOA because the following interesting observations were reported on the effects by this amine: (1) TEOA enhances homogeneous-solution CO_2 reduction as an effective additive, but not as an electron donor.[43,51] (2) Related Re(I) complexes can trap CO_2 in the presence of this amine in the dark to give TEOA-participated Re(I) carbonato complexes.[52] (3) Photocatalyzed CO_2 reduction by enzyme-loaded TiO_2 particles is largely inhibited by TEOA.[53] Interestingly, the present photocatalyzed CO_2 reduction was considerably enhanced by TEOA at 0.23 M but largely suppressed at a higher concentration (1.25 M) (Figure 8). Table 1 summarizes the effects of the additives on the photocatalyzed CO_2 reduction.

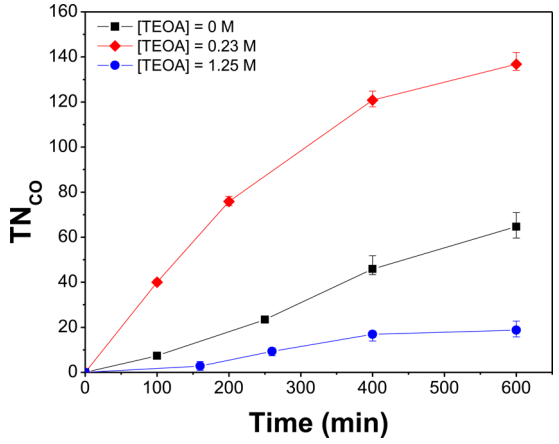

Figure 8. Plots of CO formation versus time for MOD/h-TiO_2/RePH in the absence of TEOA (■) and in the presence of TEOA at 0.23 M (red ◆) and at 1.25 M (blue ●).

Mott–Schottky Analysis of TiO_2 Nanoparticle Film under Various Conditions. As described above, the present photocatalysis systems are proved to effectively work for the reduction of CO_2, probably as the consequence of smooth electron flow from excited-singlet MOD to RePH through TiO_2. Such electron transfers should require a favorable energy alignment of the oxidation potential of excited-singlet MOD (E_{ox}*), the conduction-band edge of TiO_2 (E_{CB}), and the reduction potential of RePH (E_{red}) such that $-E_{ox}$* > $-E_{CB}$ >

DOI: 10.1021/jacs.5b08890
J. Am. Chem. Soc. 2015, 137, 13679–13690

Table 1. Additive Effects on Photocatalytic CO_2 Reduction by MOD/h-TiO_2/RePH[a]

			Li^+		Na^+	TEOA	
additive	no additive	H_2O 3% (v/v)	0.5 mM	0.1 mM	0.1 M	0.23 M	1.25 M
TN_{CO}	60	180	110	192	146	136	19

[a]Average values after 10 h irradiation.

$-E_{red}$. The reported flat-band potentials (V_{fb}) of TiO_2, which are experimentally determined representative of E_{CB}, largely vary from −0.37 to −2.25 V versus SCE depending on the sample morphologies (particle dispersions or nanoparticle films), solvents (water or organic solvents), pH for aqueous systems, and measurement methods (photoelectrochemical analysis, spectroscopy of photoelectrons, or Mott−Schottky analysis).[54−63] If the V_{fb} of our hybrid particles were −(0.37−1.02) V reported for aqueous dispersions of TiO_2 particles at pH 7,[54−56,60,61] $E^{red}_{1/2}$ of RePE (−1.34 V) would be too negative for the first electron transfer from TiO_2 to RePH to proceed (Schemes 2 and 3). On the other hand, if the reported

Scheme 2. Illustration of Electron Flow in Visible-Light-Induced CO Production on MOD/h-TiO_2/RePH

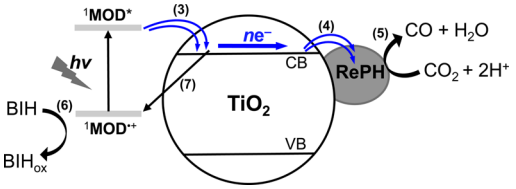

V_{fb} value of a TiO_2 nanoparticle film in DMF (−2.04 V) or in acetonitrile (−2.27 V) were adopted,[54,62] the electron injection from excited-singlet MOD (E_{ox}* ≈ −1.89 V)[32] into TiO_2 would be inefficient. In order to obtain reasonable understandings on the present observations, we carried out Mott−Schottky (MS) analysis for nanoparticle TiO_2 films on FTO electrode in thoroughly dried DMF under various conditions, which might allow us to make reasonable evaluation for relative V_{fb} values of the hybrid particles in DMF under relevant conditions; note that V_{fb} of the hybrid particles in DMF cannot be directly determined by conventional methods. From MS plots of the inverse square of observed capacitance (C_{SC}^{-2}) against applied potentials (E_{app}), V_{fb} values were calculated according to eq 2,[64] where T is the absolute temperature, $\varepsilon\varepsilon_0$ is the permittivity of TiO_2, k is the Boltzmann constant, e is the electronic charge, and N_D is the donor density of TiO_2.

$$(C_{sc})^{-2} = \frac{2\left(E_{app} - V_{fb} - \frac{kT}{e}\right)}{N_D \varepsilon\varepsilon_0 e A^2} \quad (2)$$

Figure 9 shows three different MS plots, which were taken (1) for a film that had been kept in a dry desiccator immediately after calcination of the nanoparticle film at 450 °C (dry film), (2) after keeping the dry film under ambient air for 24 h (moisture film), and (3) in the presence of 3% H_2O (wetted film); note that the hybrid particles used for the CO_2 reduction correspond to the "moisture film", since they were not subjected to calcination after the loading of the dye and catalyst. It should be noted that the V_{fb} value of the dry film (−2.25 V) is close to that reported for a nanoparticle film in DMF or acetonitrile.[62] Interestingly, however, exposure of the dry film to water atmospheres results in substantial positive shifts of V_{fb} to −1.73 V for the moisture film and further to −1.52 V for the wetted film, which should arise from adsorption of water on the surface of the TiO_2 particle film. Figure 10 shows MS plots for the dry film in the presence of $LiClO_4$ at various concentrations (see also Table S4). In this

Scheme 3. Flat-Band Potentials (V_{fb}) of TiO_2 in DMF or CH_3CN under Various Conditions Compared with Excited-State Oxidation Potential of MOD and Reduction Potential of RePE

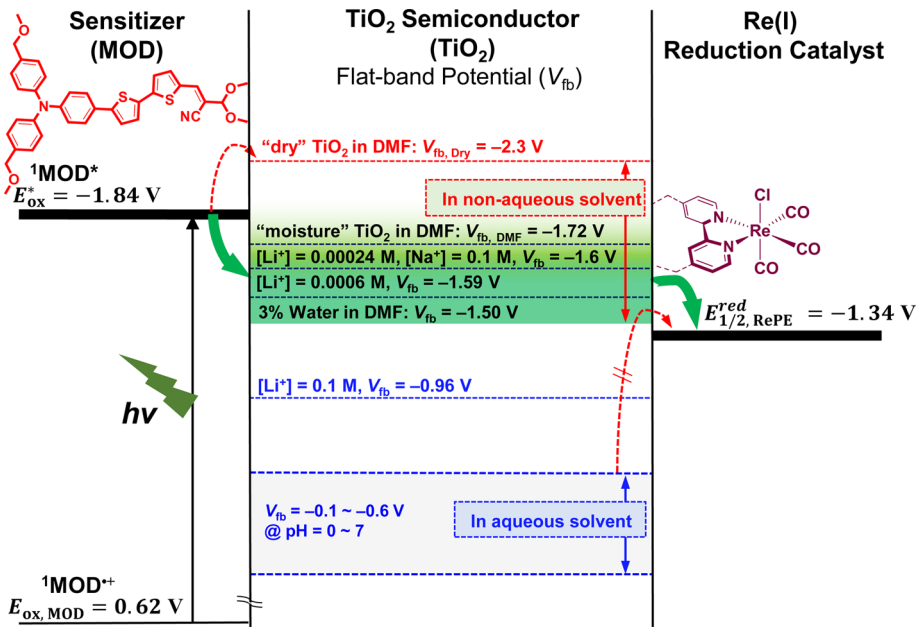

DOI: 10.1021/jacs.5b08890
J. Am. Chem. Soc. 2015, 137, 13679−13690

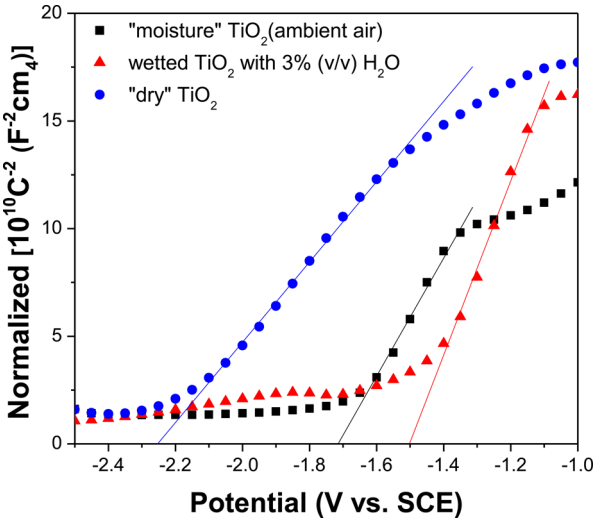

Figure 9. Mott–Schottky plots taken for dry TiO_2 nanoparticle film on FTO electrode (blue circles), after exposure of the dry film to ambient air (moisture TiO_2, black squares), and in the presence of 3% (v/v) H_2O (wetted TiO_2, red triangles). All samples are measured in DMF containing 0.1 M TBAP.

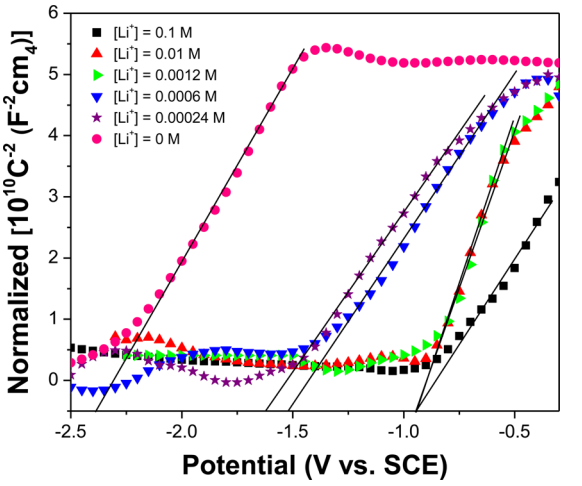

Figure 10. Mott–Schottky plots for dry TiO_2 nanoparticle film in the absence of $LiClO_4$ (pink diamonds) and in the presence of $LiClO_4$ at 0.00024 M (purple stars), 0.0006 M (blue triangles), 0.0012 M (green triangles), 0.01 M (red triangles), or 0.1 M (black squares) measured for CH_3CN solution containing 0.1 M TBAP.

experiment, acetonitrile (CH_3CN) was used as solvent because we failed to obtain reliable MS plots in DMF.[65] The dependence of V_{fb} on the concentration of $LiClO_4$ is shown in Figure 11, revealing that considerable positive shifts of V_{fb} occur by as much as ~0.6 V even at 0.24 mM and still more by ~1.18 V at >1 mM to reach a constant value. Such lowering with increase of Li^+ concentration is similar to those observed in previous reports,[54,55,78] although there is a discrepancy in a direct proportion between its concentration and V_{fb} derived from difference of type of material used, defect degrees, and measurement method.[60,61]

It is evident that the positive shifts of V_{fb} induced by water and $LiClO_4$ reveal a parallelism with the additive effects on the photocatalytic CO_2 reduction. Although the V_{fb} values obtained for the nanoparticle films are not exactly the same as those of the hybrid particles under relevant conditions, it can be easily

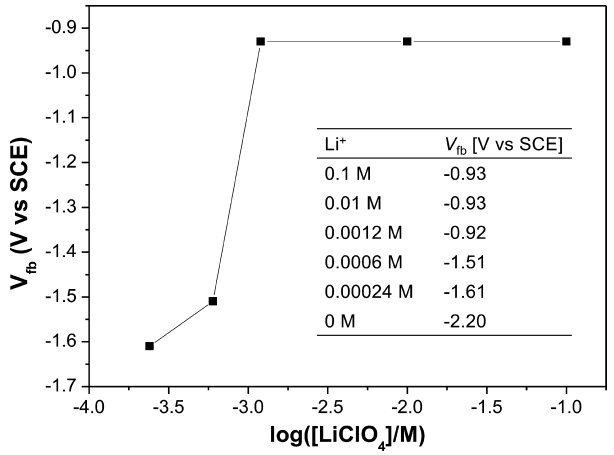

Figure 11. Flat-band potentials (V_{fb}) against log of $LiClO_4$ concentration in CH_3CN (0.1 M TBAP).

presumed that adsorption of either water or Li^+ on the TiO_2 surface should put E_{CB} toward favorable levels between E_{ox}* of MOD and E_{red} of RePH to allow smooth electron transfer from excited-singlet MOD to RePH through TiO_2 to tune optimum conditions for the photocatalytic CO_2 reduction (*vide infra*). In order to obtain possible effects of TEOA on V_{fb}, MS analysis for the dry nanoparticle film in the presence of TEOA was attempted. Unfortunately, however, only unreliable results were obtained in either DMF or CH_3CN due to detriments of the film during the measurements.

DISCUSSION

As described above, the hybrid particles do work as an effective visible-light photocatalyst for the selective reduction of CO_2 to CO with considerably high turnover numbers. Scheme 2 illustrates an outline of the major pathways for the photocatalytic reaction including processes 3–7. The initiation process is undoubtedly electron injection from excited-state MOD into the conduction band of TiO_2 (process 3). The injected electrons are transported to RePH (process 4) to drive the catalytic two-electron reduction of CO_2 on the RePH site (process 5) following the mechanism(s) suggested for homogeneous-solution photocatalysis by related Re(I) complexes (abbreviated as LReX hereafter).[40,66–70] The photocatalytic cycle for the CO_2 reduction can be completed after the recovery of MOD by the reduction of the radical cation ($MOD^{\bullet+}$) with BIH (process 6). Charge recombination of photoinjected electron with $MOD^{\bullet+}$ (process 7) is a major energy-dissipating pathway that competes with process (4) to diminish the efficiency of CO_2 reduction.

The present investigation demonstrates that the electron flow can be facilitated by tuning the reaction conditions, as shown in Scheme 3. It has been well established for dye-sensitized TiO_2 systems that the electron injection from excited dyes into TiO_2 occurs in femtosecond time regions in cases where the excited-state oxidation potential (E_{ox}*) of a dye is substantially more negative than the conduction-band edge (E_{CB}) of TiO_2.[71–76] In a previous paper, we reported that excited-singlet MOD ($^1MOD^*$) can inject an electron into TiO_2 within 1 ps in MOD-anchored TiO_2 nanoparticle films dipped into water at pH 3.[34] In this case, the flat-band potential (V_{fb}) of TiO_2 is estimated to be −(0.53–0.62) V vs SCE[54–59] which is much more positive than E_{ox}* of MOD (−1.86 V), a situation that allows the occurrence of the ultrafast electron

DOI: 10.1021/jacs.5b08890
J. Am. Chem. Soc. 2015, 137, 13679–13690

injection. In DMF, on the other hand, the V_{fb} value observed for the "dry" nanocrystalline film is −2.25 V, more negative by 0.39 eV than E_{ox}* of MOD. If we take this value as V_{fb} of the hybrid particles, the endergonic electron injection from ^{1}MOD* into "dry" TiO_2 would be much slower than the fast decay of ^{1}MOD* (∼1 ns). In the case of "moisture" or "wetted" TiO_2 or in the presence of Li^+, however, positive shifts of V_{fb} occur as much as 0.5−0.75 V so that E_{CB} might lie well below E_{ox}* of MOD. This situation is undoubtedly favorable for efficient electron injection from ^{1}MOD* into TiO_2 to overcome the decay of ^{1}MOD*. The tuning of V_{fb} by water and Li^+ should be an important contribution to the net enhancement effects of the additives on the photocatalyzed CO_2 reduction. The positive shifts should be due to hydration[76−78] or strong adsorption of small-size Li cation[79,80] on the negatively charged TiO_2 surface. Consequently, such a significant relationship between the flat-band potential of TiO_2 and the overall CO_2 conversion efficiency supports that the oxidative quenching mechanism is dominant in our hybrid system. The much less dependency of irradiance intensity also backs up the oxidative quenching mechanism at MOD and TiO_2 interface (see Figure S8 in Supporting Information).

By the same token, the smooth electron flow from ^{1}MOD* to RePH via TiO_2 requires that V_{fb} be more negative than E_{red} of RePH. This requirement appears to be satisfied for "moisture" or "wetted" TiO_2 and in the presence of Li^+ at ≤0.6 mM or Na^+ at 0.1 M in DMF. In the case of Li^+, its effects on both the photocatalyzed CO_2 reduction and the shift of V_{fb} show unique concentration dependences, such that the photocatalysis is maximally enhanced by Li^+ at 0.1 mM where $-V_{fb} > -E_{red}$, but the effect remarkably decreases at ≥10 mM where $-V_{fb} < -E_{red}$. The small-size Li cation should strongly adsorb on the TiO_2 surface to induce positive shifts of V_{fb} to appropriate degrees at low concentrations but in excess at ≥1 mM. At high concentrations of Li^+, moreover, it should be taken into consideration that Li^+ penetrates into the surface layer to form electron-trap sites.[81−83] Formation of traps distributed below the conduction-band edge should give additional energy barriers for both the electron transport in TiO_2 and the electron transfer to the RePH site. In the case of Na^+, on the other hand, a high concentration (0.1 M) is effective at both the enhancement of the photocatalyzed CO_2 reduction and a suitable shift of V_{fb} to −1.65 V,[54] perhaps due to its size being large enough to prevent excess adsorption of the cation on the TiO_2 surface as well as the cation penetration into the TiO_2 surface layer.

Similarly, the V_{fb} shift to −1.5 V in the presence of 3% water is undoubtedly an important contribution to the remarkable enhancement of photocatalyzed CO_2 reduction. However, the participation of water molecules in the chemical processes on the RePH site should be also taken into consideration because the reduction of CO_2 to CO requires the participation of a proton source, typically water, as reported for the electrochemical reduction of CO_2 catalyzed by LReX.[23,84−88] Scheme 4 shows plausible processes for the CO_2 reduction catalyzed by LReX without specifying the metal oxidation states, since the mechanistic details have not been fully explored. A 17-electron species ($LRe^{\bullet}$) formed from the one-electron reduced state ($LReX^{\bullet-}$) is likely to be responsible for the coordination of CO_2 in equilibrium with the coordination of a solvent molecule (DMF).[40,66] The follow-up processes are supposed to involve such key intermediates as a CO_2-bridged dimer complex (LReCOOReL)[66,67] and/or a metallocarboxylic acid (LReCOOH),[68−70,85] which should be formed from a putative CO_2-coordinated complex under the participation of a proton source. However, in our system, the dimer formation, LReCOOReL, would be less favorable because the reduction catalysts, RePH, are immobilized on TiO_2 surface at extremely low coverage (<0.0016).[89] The reduction product CO should be formed by hydrolysis of the key intermediate(s). Water molecules should accelerate the key chemical processes to enhance the catalytic cycle.

Scheme 4. Possible Chemical Processes for the Two-Electron Reduction of CO_2 to CO Catalyzed by a Re(I) Complex (LReX)

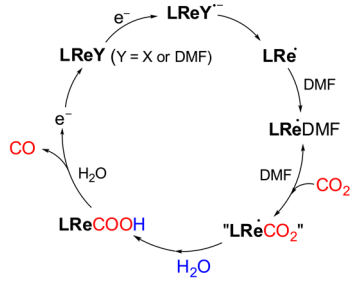

$$\mathrm{LReX} + \mathrm{CO_2} + \mathrm{TEOA} \rightleftharpoons \mathrm{LRe{-}O{-}C(=O){-}OCH_2CH_2NR_2} \quad (4)$$

The CO-formation process should involve the generation of yet unspecified complex(es) in a higher-oxidation state, which must be reduced by the second electron transfer to regenerate the starting-state complex, LRe(I)Y. Probable electron donors for the second electron transfer in homogeneous-solution photocatalysis are such long-lived reactive species as $LReY^{\bullet-}$[40,43] and a neutral radical generated from the electron donor radical cation ($SD^{\bullet+}$). In the present hybrid system, on the other hand, the second-reduction step does not necessarily require the direct participation of such reactive species but can occur with the electrons "pooled" in TiO_2, which might be long-lived[34,90,91] enough to be transferred to the RePH site ready for the second-reduction step following the above-mentioned chemical processes. The on-demand electron transfer from TiO_2 to the RePH site is a likely major origin for the persistent photocatalytic behavior of the hybrid system.

The contradictory effects of TEOA on the photocatalyzed CO_2 reduction are somewhat perplexing for us to understand. Although V_{fb} in the presence of TEOA is unavailable, the poor conversion efficiency with the addition of 1.2 M TEOA can be probably explained as a result of a negative shift of V_{fb} by electron-donating properties of TEOAs as the additive effect of ^{t}BuPy in dye-sensitized solar cells (DSSCs).[92] The retardation of the photocatalyzed reaction by 1.2 M TEOA would apparently fit the case, if TEOA would induce a shift of V_{fb} of "moisture" TiO_2 to a potential more negative than E_{ox}*. Alternatively, an excess amount of this amine would chemically deteriorate the hybrid particles. In contrast, lower concentration TEOA (0.23 M) considerably enhances the photocatalyzed CO_2 reduction, an observation that cannot be explained by possible V_{fb} shifts. Recently, it was reported that LReX efficiently traps CO_2 in the presence of TEOA to give the TEOA-bound carbonato complex ($LRe{-}OCOO{-}(CH_2)_2NR_2$; R = $(CH_2)_2OH$) (eq 4).[52] Since the CO_2 trapping occurs in equilibrium with the release of CO_2, local concentration of CO_2 in the neighborhood of the Re(I) complex might be high to accelerate the coordination of CO_2 after the first one-electron

DOI: 10.1021/jacs.5b08890
J. Am. Chem. Soc. 2015, 137, 13679−13690

reduction of the complex. We assume that the enhancement effect of TEOA at 0.23 M would mainly arise from CO_2 trapping on the RePH site.

As discussed above, the photocatalytic properties of the hybrid system can be controlled by tuning the V_{fb} of TiO_2 as well as by accelerating the chemical processes. However, the AQY for the photocalyzed CO_2 reduction is relatively low. The low value is primarily due to extensive light scattering in the opaque particle dispersion systems, which inevitably results in a poor light-harvesting efficiency. This optical drawback might be overcome, at least in part, by applying a transparent sol solution[93−95] or nanoparticle film of TiO_2 loaded with a dye and a catalyst. Another reason for the low AQY would be due to the complex chemical processes involving the "slow" coordination of CO_2 to the 17-electron species.[13,66] In particular, the second electron transfer to the RePH site should await the generation of an electron-accepting intermediate (perhaps a Re(II) species) during or after the chemical processes, so that a significant amount of electrons pooled in TiO_2 might be lost by the charge recombination with $MOD^{\bullet+}$ and/or by falling into deep traps. The former contribution can be diminished by fast reduction of $MOD^{\bullet+}$ whereas a high quality of TiO_2 would have a minimum number of deep traps. A more crucial issue is the development of efficient catalysts for the two-electron reduction of CO_2 with a least overpotential. All these subjects are directly connected with our future research target directing the creation of highly efficient, robust hybrid photocatalysts for the CO_2 reduction.

CONCLUSION

The present investigation has demonstrated that the TiO_2 hybrid system loaded with MOD as visible-light sensitizer and RePH as catalyst effectively works as a persistent photocatalyst for the selective reduction of CO_2 to CO in DMF in the presence of an electron donor (BIH) and that the photocatalytic activities can be finely tuned by such factors as (1) the TiO_2 sources with different particle sizes and morphologies, (2) the sequence in the anchoring of MOD and RePH, and (3) the concentration of such additives as water, alkali metal cations (Li^+ and Na^+), and TEOA. As the consequence, it has been achieved that a single-run photoreaction of MOD/h-TiO_2/RePH in the presence of 3% water steadily produces CO with no leveling-off tendency for 30 h to give TN_{CO} of 570, which appears to be the highest reported for heterogeneous catalytic systems to the best of our knowledge. Another typical finding is that the maximum enhancement of the photocatalytic reaction by Li^+ occurs critically at 0.1 mM accompanied by sharp decreases at higher concentrations.

Detailed Mott−Schottky analysis on V_{fb} of TiO_2 nanoparticle films under various conditions has verified that V_{fb} can be finely tuned by such additives as water, Li^+, and Na^+ to optimally align with respect to the excited-state oxidation potential of MOD and the reduction potential of RePH for the smooth electron transport from excited-singlet MOD to RePH through TiO_2. In the case of Li^+, V_{fb} shows sharp positive shifts depending on the concentration, from a value (−1.61 V) favorable for the smooth electron transport at 0.24 mM to a constant value (−0.94 V) at >1 mM being more positive than the reduction potential of Re(I) reduction center ($E^{red}_{1/2,\ RePE}$ = −1.34 V). This unique concentration dependence is in line with the concentration-dependent effect of Li^+ on the photocatalytic reaction. Thus, it has been suggested that the adjustment of V_{fb} by the additives is a major contribution to the remarkable enhancement effects of 3% water, Li^+ at 0.1 mM, and Na^+ at 0.1 M on the photocatalytic reaction due to the optimum alignment of V_{fb} for the smooth electron transport from excited-singlet MOD to RePH through TiO_2.

In addition to the optimum alignment of V_{fb}, the enhancement effect of 3% water has been suggested to involve the water-induced acceleration of chemical processes on the RePH site as well, such that water molecules adsorbed on the TiO_2 surface might participate in proton-coupled electron-transfer processes for the two-electron reduction of CO_2 to CO as well as in hydrolysis of CO_2-participated key intermediates. On the other hand, TEOA gives opposite effects on the photocatalytic reaction depending on the concentration, considerably enhancing the CO formation at 0.23 M in contrast to a large inhibition of the reaction at 1.2 M. It has been suggested that the enhancement of the reaction at 0.23 M would be due to CO_2 trapping by RePH under the participation of TEOA, while high-concentration TEOA would induce an excess negative shift of V_{fb} unfavorable for the electron injection from excited-singlet MOD to TiO_2 and/or would deteriorate the hybrid particles. The present investigation provides a potential tactics for the construction of robust ternary hybrid systems consisting of a semiconductor, a visible-light harvesting dye, and a molecular catalyst for the efficient reduction of CO_2.

EXPERIMENTAL SECTION

General Procedures. All reagents were purchased from Aldrich and used without further purification. All manipulations were performed under a dry nitrogen or argon atmosphere by using standard Schlenk techniques. *N*,*N*-Dimethylformamide (DMF) was distilled from calcium hydride and stored over molecular sieves. Acetonitrile (CH_3CN) was refluxed over and distilled from phosphorus pentoxide (P_2O_5) before use. The ^1H and ^{13}C NMR spectra were recorded on a Varian Mercury 300 spectrometer operating at 300.1 and 75.4 MHz, respectively, for DMF-d_7 solutions. Proton and carbon chemical shifts were referenced relative to the corresponding solvent signals, δ H 2.75, 2.92, and 8.03 and δ C 29.76, 34.89, and 163.15 of DMF-d_7. The absorption and photoluminescence spectra were recorded on a Shimadzu UV-3101PC UV/vis/NIR scanning spectrophotometer, a Agilent Technologies Cary 5000 UV−vis−NIR spectrophotometer, and a VARIAN Cary Eclipse fluorescence spectrophotometer, respectively. The diffuse reflectance UV−vis absorption spectra of powder samples were recorded on a Scinco spectrophotometer S-3100. The IR spectra were taken on a Cary 660 FTIR spectrometer. Cyclic voltammetry (CV) measurements were carried out for DMF solutions of the rhenium complexes or the dye (1 mM) in the presence of tetrabutylammonium perchlorate (0.1 M) at room temperature using a BAS 100B electrochemical analyzer equipped with a glassy carbon or a Pt working electrode, a platinum wire counter electrode, and an Ag|$AgNO_3$ (0.1 M) or an Ag|AgCl reference. All potential values except using an Ag|AgCl reference were calibrated against a ferrocenium/ferrocene (Fc^+/Fc) redox couple (−0.63 V). The Mott−Schottky measurements were carried out for DMF and CH_3CN solutions of the TiO_2 working electrode in the presence of tetrabutylammonium perchlorate (0.1 M) at room temperature using a CH Instruments CHI660D equipped with a platinum wire counter electrode and a SCE reference. Measurements of particle sizes were used by Microtrac UPA 150 to apply dynamic light scattering Doppler shift controlled referenced. Elemental analysis (Carlo Erba Instruments CHNS-O EA1108 analyzer) and HR-MS (FAB) (Jeol LTD JMS-HX110/110A) were performed by the Ochang branch of the Korean Basic Science Institute.

Preparation of Dye-Sensitized TiO_2 Catalyst. The [001] facet exposed TiO_2, which had been prepared according to the published method,[38] was treated with 0.1 M NaOH aqueous solution to give s-TiO_2.[39] The alkaline treatment was indispensable for efficient deposition of ReC and dye on the particles because the deposition

DOI: 10.1021/jacs.5b08890
J. Am. Chem. Soc. 2015, 137, 13679−13690

of RePH and dye was poor on the fluorinated surface of the as-prepared [001] TiO_2. Commercially available Hombikat UV-100 (h-TiO_2), Degussa P25 (d-TiO_2), and s-TiO_2 were thoroughly washed with distilled water, ultrasonically treated in water, separated by centrifugation, and then dried in an oven under N_2. The TiO_2 particles (0.1 g) were stirred overnight in an CH_3CN/*tert*-butanol solution of RePH (1 μmol) and then subjected to centrifugation. The collected solids were washed with the solvent and then dried in an oven under N_2. The Re(I) complex-deposited TiO_2 powders (0.1 g) were dispersed into an CH_3CN/*tert*-butanol solution of dye (15 μmol) and allowed to stand overnight under stirring. The photocatalysts (RePH/TiO_2/MOD) were separated by centrifugation, washed with CH_3CN/*tert*-butanol, dried in an oven (70 °C), and stored under N_2 in the dark. The preparation of MOD/TiO_2/RePH was performed by the initial loading of dye on the TiO_2 particles followed by treatment with a CH_3CN/*tert*-butanol solution of RePH, while each procedure for dye or RePH loading was identical to that described above for RePH/TiO_2/MOD. UV−vis absorption spectroscopy confirmed that each supernatant separated after centrifugation of the MOD- and RePH-treated suspensions shows negligible absorption of MOD or RePH.

Photocatalyzed CO_2 Reduction. Suspensions of RePH/TiO_2/MOD or MOD/TiO_2/RePH particles (10 mg with 0.1 μmol of RePH and 1.5 μmol of MOD) in 3 mL of DMF containing BIH (0.1 M) were placed in a quartz cell (1 cm pass length; 6.0 mL total volume), bubbled with CO_2 for 30 min, sealed with a septum, and then irradiated using a xenon lamp while stirring (450 W, model 66924, Newport Corporation); the incident light (λ > 420 nm) was obtained by passing the light from the xenon lamp through a water layer of a 10 cm path length and a glass light filter. The amounts of CO evolved in the overhead space of the cell were determined by gas chromatography (HP6890A GC equipped with a TCD detector) using a SUPELCO CarboxenTM 1010 PLOT fused silica capillary column. The apparent quantum yield Φ_{CO} for CO_2 reduction was determined for the MOD/h-TiO_2/RePH suspensions, a band-pass filter (415−450 nm) was used to isolate the 436 nm light form the emission light of a high-pressure mercury lamp (1000 W, model 6171, Newport Corporation), and the incident light flux was determined by using a 0.2 M ferrioxalate actinometer solution.[96]

■ ASSOCIATED CONTENT

Supporting Information

The Supporting Information is available free of charge on the ACS Publications website at DOI: 10.1021/jacs.5b08890.

Results of photophysical (UV−vis absorption and photoluminescence spectra) and electrochemical data (cyclic voltammogram) of samples, plots of CO formation versus time for hybrid catalysts, XRD pattern of TiO_2 samples, and GC spectrum of gas in the reaction vessel (PDF)

■ AUTHOR INFORMATION

Corresponding Authors

*E-mail hjson@korea.ac.kr.
*E-mail jjpac@korea.ac.kr.
*E-mail sangok@korea.ac.kr.

Notes

The authors declare no competing financial interest.

■ ACKNOWLEDGMENTS

We acknowledge support from Basic Science Research Program through the National Research Foundation of Korea (NRF) funded by the Ministry of Education (NRF-2014R1A6A1030732) and the Ministry of Science, ICT & Future Planning (2014R1A1A1007625).

■ ABBREVIATIONS

MOD, (*E*)-3-[5-(4-(*p*,*p*′-bis(R-phenyl)amino)phenyl)-2,2′-bithiophen-2′-yl]-2-cyanoacrylic acid (R = CH_2OCH_3); RePH, (4,4′-bis(methylphosphonic acid)-2,2′-bipyridine)-$Re^I(CO)_3Cl$; BIH, 1,3-dimethyl-2-phenyl-1,3-dihydrobenzimidazole.

■ REFERENCES

(1) Lal, R. *Energy Environ. Sci.* **2008**, *1*, 86−100.
(2) Roy, S. C.; Varghese, O. K.; Paulose, M.; Grimes, C. A. *ACS Nano* **2010**, *4*, 1259−1278.
(3) BP statistical Review of World Energy 2015, Spencer Dale, July 2015; http://www.bp.com/en/global/corporate/about-bp/energy-economics/statistical-review-of-world-energy.html.
(4) Appel, A. M.; Bercaw, J. E.; Bocarsly, A. B.; Dobbek, H.; DuBois, D. L.; Dupuis, M.; Ferry, J. G.; Fujita, E.; Hille, R.; Kenis, P. J. A.; Kerfeld, C. A.; Morris, R. H.; Peden, C. H. F.; Portis, A. R.; Ragsdale, S. W.; Rauchfuss, T. B.; Reek, J. N. H.; Seefeldt, L. C.; Thauer, R. K.; Waldrop, G. L. *Chem. Rev.* **2013**, *113*, 6621−6658.
(5) Aresta, M. *Carbon Dioxide as Chemical Feedstock*; Wiley-VCH: Weinheim, 2010.
(6) Doherty, M. D.; Grills, D. C.; Muckerman, J. T.; Polyansky, D. E.; Fujita, E. *Coord. Chem. Rev.* **2010**, *254*, 2472−2482.
(7) Berardi, S.; Drouet, S.; Francas, L.; Gimbert-Surinach, C.; Guttentag, M.; Richmond, C.; Stoll, T.; Llobet, A. *Chem. Soc. Rev.* **2014**, *43*, 7501−7519.
(8) Knör, G. *Coord. Chem. Rev.* **2015**, *304*−*305*, 102−108.
(9) Fujita, E. *Coord. Chem. Rev.* **1999**, *185*-*186*, 373−384.
(10) Schwarz, H. A.; Dodson, R. W. *J. Phys. Chem.* **1989**, *93*, 409−414.
(11) Fujita, E.; Brunschwig, B. S. Catalysis of Electron Transfer, Heterogeneous Systems, Gas Phase Systems. In *Electron Transfer in Chemistry*; Balzani, V., Ed.; Wiley-VCH: Weinheim, Germany, 2001; Vol. *4*, pp 88−126.
(12) Lamy, E.; Nadjo, L.; Savéant, J. M. *J. Electroanal. Chem. Interfacial Electrochem.* **1977**, *78*, 403−407.
(13) Morris, A. J.; Meyer, G. J.; Fujita, E. *Acc. Chem. Res.* **2009**, *42*, 1983−1994.
(14) Yui, T.; Tamaki, Y.; Sekizawa, K.; Ishitani, O. *Top. Curr. Chem.* **2011**, *303*, 151−184.
(15) Alibabai, L.; Luo, H.; House, R. L.; Hoeltz, P. G.; Meyer, T. J. *J. Mater. Chem. A* **2013**, *1*, 4133−4145.
(16) Savéant, J.-M. *Chem. Rev.* **2008**, *108*, 2348−2378.
(17) Benson, E. E.; Kubiak, C. P.; Sathrum, A. J.; Smieja, J. M. *Chem. Soc. Rev.* **2009**, *38*, 89−99.
(18) Costentin, C.; Robert, M.; Savéant, J.-M. *Chem. Soc. Rev.* **2013**, *42*, 2423−2436.
(19) Qiao, J.; Liu, Y.; Hong, F.; Zhang, J. *Chem. Soc. Rev.* **2014**, *43*, 631−675.
(20) Tanaka, K.; Ooyama, D. *Coord. Chem. Rev.* **2002**, *226*, 211−218.
(21) Takeda, H.; Koike, K.; Morimoto, T.; Inumaru, H.; Ishitani, O.; van Eldik, R.; Stochel, G. *Adv. Inorg. Chem.* **2011**, *63*, 137−186.
(22) Hawecker, J.; Lehn, J.-M.; Ziessel, R. *J. Chem. Soc., Chem. Commun.* **1983**, 536−538.
(23) Hawecker, J.; Lehn, J.-M.; Ziessel, R. *Helv. Chim. Acta* **1986**, *69*, 1990−2012.
(24) Kumar, B.; Llorente, M.; Froehlich, J.; Dang, T.; Sathrum, A.; Kubiak, C. P. *Annu. Rev. Phys. Chem.* **2012**, *63*, 541−569.
(25) Song, W.; Chen, Z.; Glasson, C. R. K.; Hanson, K.; Luo, H.; Norris, M. R.; Ashford, D. L.; Concepcion, J. J.; Brennaman, K. K.; Meyer, T. J. *ChemPhysChem* **2012**, *13*, 2882−2890.
(26) Woolerton, T. W.; Sheard, S.; Reisner, E.; Pierce, E.; Ragsdale, S. W.; Armstrong, F. A. *J. Am. Chem. Soc.* **2010**, *132*, 2132−2133.
(27) Woolerton, T. W.; Sheard, S.; Pierce, E.; Ragsdale, S. W.; Armstrong, F. A. *Energy Environ. Sci.* **2011**, *4*, 2393−2399.
(28) Windle, C. D.; Pastor, E.; Reynal, A.; Whitwood, A. C.; Vaynzof, Y.; Durrant, J. R.; Perutz, R. N.; Reisner, E. *Chem. - Eur. J.* **2015**, *21*, 3746−3754.

DOI: 10.1021/jacs.5b08890
J. Am. Chem. Soc. 2015, 137, 13679−13690

(29) Sato, S.; Morikawa, T.; Saeki, S.; Kajino, T.; Motohiro, T. *Angew. Chem., Int. Ed.* **2010**, *49*, 5101−5105.
(30) Arai, T.; Tajima, S.; Sato, S.; Uemura, K.; Morikawa, T.; Kajino, T. *Chem. Commun.* **2011**, *47*, 12664−12666.
(31) Sato, S.; Arai, T.; Morikawa, T.; Uemura, K.; Suzuki, T. M.; Tanaka, H.; Kajino, T. *J. Am. Chem. Soc.* **2011**, *133*, 15240−15243.
(32) Ha, E.-G.; Chang, J.-A.; Byun, S.-M.; Pac, C.; Jang, D.-M.; Park, J.; Kang, S. O. *Chem. Commun.* **2014**, *50*, 4462−4464.
(33) Lee, S.-H.; Park, Y.; Wee, K.-R.; Son, H.-J.; Cho, D. W.; Pac, C.; Choi, W.; Kang, S. O. *Org. Lett.* **2010**, *12*, 460−463.
(34) Han, W.-S.; Wee, K.-R.; Kim, H.-Y.; Pac, C.; Nabetani, Y.; Yamamoto, D.; Shimada, T.; Inoue, H.; Choi, H.; Cho, K.; Kang, S. O. *Chem. - Eur. J.* **2012**, *18*, 15368−15381.
(35) Angelici, R. J.; Kruse, A. E. *J. Organomet. Chem.* **1970**, *22*, 461−471.
(36) Yi, X.; Zhao, J.; Sun, J.; Guo, S.; Zhang, H. *Dalton Trans.* **2013**, *42*, 2062−2074.
(37) Zhu, X.-Q.; Zhang, M.-T.; Yu, A.; Wang, C.-H.; Cheng, J.-P. *J. Am. Chem. Soc.* **2008**, *130*, 2501−2516.
(38) Han, X.; Kuang, Q.; Jin, M.; Xie, Z.; Zheng, L. *J. Am. Chem. Soc.* **2009**, *131*, 3152−3153.
(39) Wang, Q.; Chen, C.; Zhao, D.; Ma, W.; Zhao, J. *Langmuir* **2008**, *24*, 7338−7345.
(40) Takeda, H.; Koike, K.; Inoue, H.; Ishitani, O. *J. Am. Chem. Soc.* **2008**, *130*, 2023−2031.
(41) Wang, C.; Xie, Z.; deKrafft, K. E.; Lin, W. *J. Am. Chem. Soc.* **2011**, *133*, 13445−13454.
(42) Liu, C.; Dubois, K. D.; Lois, M. E.; Vorushilov, A. S.; Li, G. *ACS Catal.* **2013**, *3*, 655−662.
(43) Gholamkhass, B.; Mametsuka, H.; Koike, K.; Tanabe, T.; Furue, M.; Ishitani, O. *Inorg. Chem.* **2005**, *44*, 2326−2336.
(44) Bian, Z.-Y.; Sumi, K.; Furue, M.; Sato, S.; Koike, K.; Ishitani, O. *Dalton Trans.* **2009**, 983−993.
(45) Tamaki, Y.; Watanabe, K.; Koike, K.; Inoue, H.; Morimoto, T.; Ishitani, O. *Faraday Discuss.* **2012**, *155*, 115−127.
(46) Tamaki, Y.; Koike, K.; Morimoto, T.; Ishitani, O. *J. Catal.* **2013**, *304*, 22−28.
(47) Morimoto, T.; Nishiura, C.; Tanaka, M.; Rohacova, J.; Nakagawa, Y.; Funada, Y.; Koike, K.; Yamamoto, Y.; Shishido, S.; Kojima, T.; Saeki, T.; Ozeki, T.; Ishitani, O. *J. Am. Chem. Soc.* **2013**, *135*, 13266−13269.
(48) Kutal, C.; Weber, M. A.; Ferraudi, G.; Geiger, D. *Organometallics* **1985**, *4*, 2161−2166.
(49) Kutal, C.; Corbin, A. J.; Ferraudi, G. *Organometallics* **1987**, *6*, 553−557.
(50) Ishitani, O.; Namura, I.; Yanagida, S.; Pac, C. *J. Chem. Soc., Chem. Commun.* **1987**, 1153−1154.
(51) Ishitani, O.; Yanagida, S.; Takamuku, S.; Pac, C. *J. Org. Chem.* **1987**, *52*, 2790−2796.
(52) Morimoto, T.; Nakajima, T.; Sawa, S.; Nakanishi, R.; Imori, D.; Ishitani, O. *J. Am. Chem. Soc.* **2013**, *135*, 16825−16828.
(53) Chaudhary, Y. S.; Woolerton, T. W.; Allen, C. S.; Warner, J. H.; Pierce, E.; Ragsdale, S. W.; Armstrong, F. A. *Chem. Commun.* **2012**, *48*, 58−60.
(54) Redmond, G.; Fitzmaurice, D. F. *J. Phys. Chem.* **1993**, *97*, 1426−1430.
(55) Rothenberger, G.; Fitzmaurice, D.; Grätzel, M. *J. Phys. Chem.* **1992**, *96*, 5983−5986.
(56) Ward, M. D.; White, J. M.; Bard, A. J. *J. Am. Chem. Soc.* **1983**, *105*, 27−31.
(57) Lyon, L. A.; Hupp, J. T. *J. Phys. Chem. B* **1999**, *103*, 4623−4628.
(58) O'Regan, B.; Moser, J.; Anderson, M.; Grätzel, M. *J. Phys. Chem.* **1990**, *94*, 8720−8726.
(59) Dung, D.; Ramsden, J.; Grätzel, M. *J. Am. Chem. Soc.* **1982**, *104*, 2977−2985.
(60) Di Paola, A.; Bellardita, M.; Ceccato, R.; Palmisano, L.; Parrino, F. *J. Phys. Chem. C* **2009**, *113*, 15166−15174.
(61) Kandiel, T. A.; Feldhoff, A.; Robben, L.; Dillert, R.; Bahnemann, D. W. *Chem. Mater.* **2010**, *22*, 2050−2060.
(62) Zhang, C.; Jiang, L.; Mo, L.; Huang, Y.; Xiao, S.; Hu, L.; Chen, S.; Huo, Z.; Kong, F.; Dai, S. *J. Electroanal. Chem.* **2015**, *736*, 107−111.
(63) Wang, G.; Wang, Q.; Lu, W.; Li, J. *J. Phys. Chem. B* **2006**, *110*, 22029−22034.
(64) van de Krol, R.; Goossens, A.; Schoonman, J. *J. Electrochem. Soc.* **1997**, *144*, 1723−1727.
(65) For the MS measurement in DMF, it was difficult to get a reliable/exact data because the measured V_{fb} value is significantly fluctuant (continuously lowered) with water adsorption of DMF solvent (derived from the significant hygroscopic nature of DMF) over time during MS measurement. For this reason, we cannot proceed the MS measurement in DMF and, instead, we did in CH_3CN, whose water adsorption ability is relatively nominal (thus resulting in almost constant values on measurement).
(66) Hayashi, Y.; Kita, S.; Brunschwig, B. S.; Fujita, E. *J. Am. Chem. Soc.* **2003**, *125*, 11976−11987.
(67) Agarwal, J.; Fujita, E.; Schaefer, H. F.; Muckerman, J. T. *J. Am. Chem. Soc.* **2012**, *134*, 5180−5186.
(68) Gibson, D. H.; Yin, X. *J. Am. Chem. Soc.* **1998**, *120*, 11200−11201.
(69) Gibson, D. H.; Yin, X.; He, H.; Mashuta, M. S. *Organometallics* **2003**, *22*, 337−346.
(70) Kou, Y.; Nabetani, Y.; Masui, D.; Shimada, T.; Takagi, S.; Tachibana, H.; Inoue, H. *J. Am. Chem. Soc.* **2014**, *136*, 6021−6030.
(71) Miller, R. J. D.; McLendon, G. L.; Nozik, A. J.; Schmickler, W.; Willing, F. *Surface Electron Transfer Processes*; VCH Publishers: New York, 1995.
(72) Hagfeldt, A.; Grätzel, M. *Chem. Rev.* **1995**, *95*, 49−68.
(73) Yan, S. G.; Hupp, J. T. *J. Phys. Chem.* **1996**, *100*, 6867−6870.
(74) Hamann, T. W.; Jensen, R. A.; Martinson, A. B. F.; Van Ryswyk, H.; Hupp, J. T. *Energy Environ. Sci.* **2008**, *1*, 66−78.
(75) Brennaman, M. K.; Patrocinio, A. O. T.; Song, W.; Jurss, J. W.; Concepcion, J. J.; Hoertz, P. G.; Traub, M. C.; Murakami Iha, N. Y.; Meyer, T. J. *ChemSusChem* **2011**, *4*, 216−227.
(76) She, C.; Guo, J.; Lian, T. *J. Phys. Chem. B* **2007**, *111*, 6903−6912.
(77) Zhu, K.; Jang, S.-R.; Frank, A. J. *Energy Environ. Sci.* **2012**, *5*, 9492−9495.
(78) Enright, B.; Redmond, G.; Fitzmaurice, D. *J. Phys. Chem.* **1994**, *98*, 6195−6200.
(79) Koops, S. E.; O'Regan, B. C.; Barnes, P. R. F.; Durrant, J. R. *J. Am. Chem. Soc.* **2009**, *131*, 4808−4818.
(80) Kelly, C. A.; Farzad, F.; Thompson, D. W.; Stipkala, J. M.; Meyer, G. J. *Langmuir* **1999**, *15*, 7047−7054.
(81) Fredin, K.; Nissfolk, J.; Boschloo, G.; Hagfeldt, A. *J. Electroanal. Chem.* **2007**, *609*, 55−60.
(82) Zhang, J.; Steigerwald, M.; Brus, L.; Friesner, R. A. *Nano Lett.* **2014**, *14*, 1785−1789.
(83) Zhang, J.; Hughes, T. F.; Steigerwald, M.; Brus, L.; Friesner, R. A. *J. Am. Chem. Soc.* **2012**, *134*, 12028−12042.
(84) Portenkirchner, E.; Kianfar, E.; Sariciftci, N. S.; Knör, G. *ChemSusChem* **2014**, *7*, 1347−1351.
(85) Smieja, J. M.; Benson, E. E.; Kumar, B.; Grice, K. A.; Seu, C. S.; Miller, A. J. M.; Mayer, J. M.; Kubiak, C. P. *Proc. Natl. Acad. Sci. U. S. A.* **2012**, *109*, 15646−15650.
(86) Keith, J. A.; Grice, K. A.; Kubiak, C. P.; Carter, E. A. *J. Am. Chem. Soc.* **2013**, *135*, 15823−15829.
(87) Smieja, J. M.; Kubiak, C. P. *Inorg. Chem.* **2010**, *49*, 9283−9289.
(88) Wong, K.-Y.; Chung, W.-H.; Lau, C.-P. *J. Electroanal. Chem.* **1998**, *453*, 161−170.
(89) The degree of coverage of RePH on h-TiO_2 surface is calculated using the following method: 4×10^{-4} m^2 (area of RePH adsorbed on 10 mg of h-TiO_2)/0.25 m^2 (surface area of 10 mg of h-TiO_2) = 1/625 (0.0016).
(90) Szczepankiewicz, S. H.; Colussi, A. J.; Hoffmann, M. R. *J. Phys. Chem. B* **2000**, *104*, 9842−9850.
(91) Szczepankiewicz, S. H.; Moss, J. A.; Hoffmann, M. R. *J. Phys. Chem. B* **2002**, *106*, 7654−7658.

DOI: 10.1021/jacs.5b08890
J. Am. Chem. Soc. 2015, 137, 13679−13690

(92) Zhang, S.; Yang, X.; Zhang, K.; Chen, H.; Yanagida, M.; Han, L. *Phys. Chem. Chem. Phys.* **2011**, *13*, 19310−19313.
(93) Burunkaya, E.; Akarsu, M.; Camurlu, H. E.; Kesmez, O.; Yesil, Z.; Asilturk, M.; Arpac, E. *Appl. Surf. Sci.* **2013**, *265*, 317−323.
(94) Gonçalves, R. H.; Schreiner, W. H.; Leite, E. R. *Langmuir* **2010**, *26*, 11657−11662.
(95) Katsumata, K.-I.; Ohno, Y.; Tomita, K.; Taniguchi, T.; Matsushita, N.; Okada, K. *ACS Appl. Mater. Interfaces* **2012**, *4*, 4846−4852.
(96) Braun, A. M.; Maurette, M.-T.; Oliveros, E. *Photochemical Technology*; Wiley & Sons: New York, 1991; pp 76−80 and references therein.

DOI: 10.1021/jacs.5b08890
J. Am. Chem. Soc. 2015, 137, 13679−13690